

NANOCRYSTALLINE HARDYSTONITE SYNTHESIZED BY SOLID
STATE PROCESS AS A NOVEL BIO-CERAMIC FOR MEDICAL
PURPOSES; PREPARATION AND CHARACTERIZATION

E. Karamian¹, H. Gheisari²

¹ Islamic Azad University – Najafabad Branch
Advanced Materials Research Center
Najafabad, Isfahan, Iran
ebkaramian91@gmail.com
ekaramian@pmt.iaun.ac.ir

² Islamic Azad University– Lenjan Branch
Department of Mechanical and Industrial
Isfahan, Iran

Accepted October 19, 2015

Abstract

In this study, Hardystonite powder ($\text{Ca}_2\text{ZnSi}_2\text{O}_7$) was synthesized by mechanical activation method as a solid state process. Specimens were composed of a blend of pure calcite, silica amorphous and ZnO with 50, 30 and 20 wt. %, respectively. These powders were milled by high energy ball mill using ball-to-powder ratio 10 : 1 and rotation speed (600 rpm) for 5 and 10 h. Then, the mixtures mechanical activated have been heated at 1100 °C for 3 h. XRD, SEM and BET performed on the samples to characterize. According to XRD results, the sample milled for 10 h just indicated the Hardystonite phase, with crystal size about 40 nm, while the sample milled for 5 h illustrate Hardystonite phase along with several phases. Based on energy transfer analysis, the energy amount transferred to the starting materials is 11.2 MJ /g for 10 h, causes the synthesis temperature reduces to 1100 °C.

1. Introduction

Previous studies showed that some Ca, Si containing bioactive glass, glass-ceramics and ceramics were biocompatible [1 – 3] and could induce hydroxyapatite (HAp) formation in body fluid environment [4]. Zn was reported to be involved in bone metabolism [5]. Zn could stimulate bone formation and increase bone protein, calcium content, and alkaline phosphatase activity in humans and animals [6]. Hardystonite ($\text{Ca}_2\text{ZnSi}_2\text{O}_7$) is a mineral containing Ca, Zn, and Si, with a melting temperature of 1425 °C and a density of 3.40 g / cm³, and so far has no important industrial applications. Considering chemical composition, Hardystonite might be biocompatible and used as biomaterials. To our knowledge, there was no report about preparation of Hardystonite ceramic [7]. Recently, silicate based bioceramics such as wollastonite (CaSiO_3) [8, 9], dicalcium silicate (Ca_2SiO_4) [10], bredigite ($\text{Ca}_7\text{MgSi}_4\text{O}_{16}$) [11] and Akermanite ($\text{Ca}_2\text{MgSi}_2\text{O}_7$) [12] have showed excellent in vitro bioactivity, mechanical property and biocompatibility. Most attractive is that in vivo studies also proved that silicate bioceramics could promote new bone formation.

Zinc has a stimulatory effect on bone formation and mineralization and moreover, it inhibits osteoclastic bone restoration [13]. Previously, the study of Zn-doped CaSiO_3 [14] demonstrated that the incorporation of Zn could promote human bone osteoblastic-like cells proliferation and ALP activity. Recent studies revealed that some zinc-containing silicate ceramics such as willemite (Zn_2SiO_4) [15] and Hardystonite ($\text{Ca}_2\text{ZnSi}_2\text{O}_7$) [14, 16 – 18] were also able to enhance one marrow stem cell proliferation and differentiation. In this study, Hardystonite powder was synthesized by solid state method. The starting materials were mechanical activated by high energy ball milling and compacted by uniaxial pressing then the powder mixture milled was heated at high temperature, 1100 °C. The aim of the present work was to investigate characterization of nanostructure Hardystonite ceramic as opposed to previous studies. The results of this paper can be used for further researches and it would promote the possibility of usages of nanostructure Hardystonite ceramic in orthopaedic applications.

In this study, energy transferred to the starting materials mixture, causes the materials to be mechanically activated and leads to the synthesis temperature of Hardystonite reduces to low temperature.

2. Materials and methods

Hardystonite was synthesized by pure calcite (Merck, 99%), amorphous pure silica and pure zinc oxide (ZnO, 98 %) with 50, 30 and 20 wt. %, respectively. The powder mixture was milled by high energy ball mill, ball-to-powder ratio 10 : 1 and rotation speed 600 rpm, for 5 and 10 h. Then, the mixture milled has been heated at 1100 °C for 3 h in muffle furnace at air atmosphere. Phase structure analysis was carried out by X-ray diffraction (XRD) (Philips X'Pert-MPD diffractometer with Cu K α radiation ($\lambda_1 = 0.15418$ nm) over the 2θ range of 10 – 90 deg.). The obtained experimental patterns were compared to the standards compiled by the Joint Committee on Powder Diffraction and Standards (JCDPS) which involved card # 01-072-1 for hardystonite phase. Hardystonite crystalline size of was determined using XRD patterns and modified Scherrer equation. Scanning electron microscopy (SEM) analyses evaluations were performed using a Philips XL30 to investigate the morphology. SEM micrograph was performed using a LEO 435 VP to investigate the morphology. SEM samples coated with Au by sputter spraying, low vacuum and 100 – 120 V accelerating voltage, for 120 s. The powder prepared coated with Au by spraying, low vacuum and 25 kV accelerating voltage. Mechanical activation has been done by PE2 high energy planetary ball mill machine for 5 and 10 h. The specific surface area of powder mixture milled has been done by BET technique, Kelvin B100.

2.1. The modified Scherrer equation

The purpose of modified Scherrer equation given in this paper is to provide a new approach to the kind of using Scherrer equation, so that a least squares method can be applied to minimize the sources of errors. Modified Scherrer equation plots $\ln \beta$ against $\ln (1 / \text{Cos } \theta)$ and obtains the intercept of a least squares line regression, $\ln(K\lambda/L)$, from which a single value of L is obtained through all of the available peaks. The modified Scherrer equation can provide the advantage of decreasing the sum of absolute values of errors, $\sum(\pm\Delta\ln\beta)^2$, and producing a single line through the points to give a single value of intercept $\ln(K\lambda/L)$ [19].

2.2. Energy transfer

Figure 1 shows the schematic diagram of the planetary ball mill and the vial: indicating by W_p and W_v the absolute angular velocity of the plate of the mill and of one vial and by R_p and R_v the vectorial distances from the centre of the mill to the centre of the vial and from the centre of the vial to its periphery (vial radius), it can be shown the absolute velocity of one ball leaving the wall is given by:

$$V_b = [(W_p R_p)^2 + W_v^2 (R_v - d_b / 2)^2 (1 - 2W_v / W_p)]^{1/2}, \quad (1)$$

the velocity of the ball with d_b diameter, after the hits, equals that of the inner wall and can be expressed as follow:

$$V_s = [(W_p R_p)^2 + W_v^2 (R_v - d_b / 2)^2 + 2W_p W_v R_p (R_v - d_b / 2)]^{1/2}. \quad (2)$$

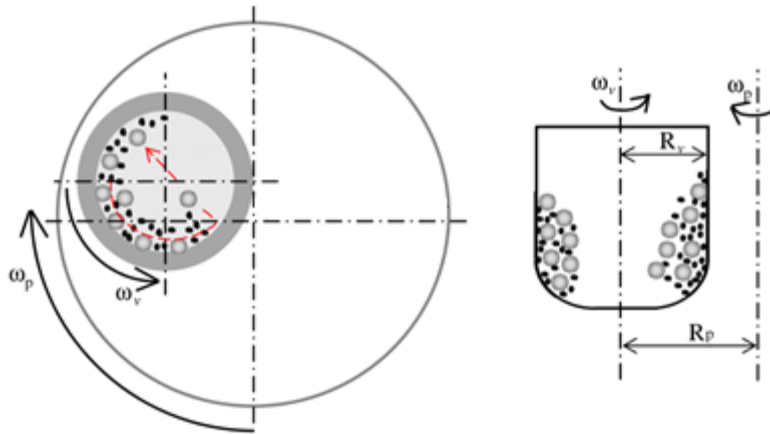


Figure 1. The schematic diagram of the planetary ball mill and the vial.

We have to consider now the mechanism of energy transfer. When the ball is thrown, it possesses the kinetic energy:

$$E = 1/2 m_b V_b^2. \quad (3)$$

After a short succession of hits, during which decreasing fractions of kinetic energy are released, the balls residual energy becomes:

$$E = 1/2 m_b V_s^2 \quad (4)$$

and the total energy released by the ball during the series of collision events is given by:

$$\Delta E_b = E_b - E_s = -m_b [W_v^3 (R_v - d_b / 2) / W_p + W_p W_v R_p] (R_v - d_b / 2). \quad (5)$$

with the assumption that the total energy transferred by the planetary mill per gram of reactant mixture and required to synthesis of nano-structure powders is a constant value, the Burgio model defines this amount of energy by the following expression:

$$E_t / g = \frac{(N_b \varphi_b f_b K_a m_b) [W_v^3 (R_v - d_b / 2) / W_p + W_p W_v R_p] (R_v - d_b / 2) t}{m_{ch}} = A (J / g), \quad (6)$$

where N_b is the number of balls; K_a is a constant that accounts for the elasticity of collisions, and a value of 1 represents perfectly inelastic collisions; m_{ch} is the mass of the powder charge; and t is the synthesis time measured. φ_b is a parameter that accounts for the degree of filling of the vial; f_b is the frequency with which the balls are launched against the opposite wall of the vial.

$$\varphi_b = 1 - \left(\frac{d_b^3 N_b}{\pi R_v^2 H_v} \right)^\varepsilon, \quad (7)$$

$$f_b = \frac{K(W_p - W_v)}{2\pi}, \quad (8)$$

$$m_b = \frac{\pi\rho_b d_b^3}{6}. \quad (9)$$

where H_v, ρ_b are respectively the height of the vial and the density of balls? K is a proportionality constant and is approximately equal to unity and ε is a parameter called ball diameter distribution coefficient depending on the balls diameter [20].

3. Results

3.1. SEM micrographs

Figures 1 and 2 show the SEM micrographs the materials milled before and after heating.

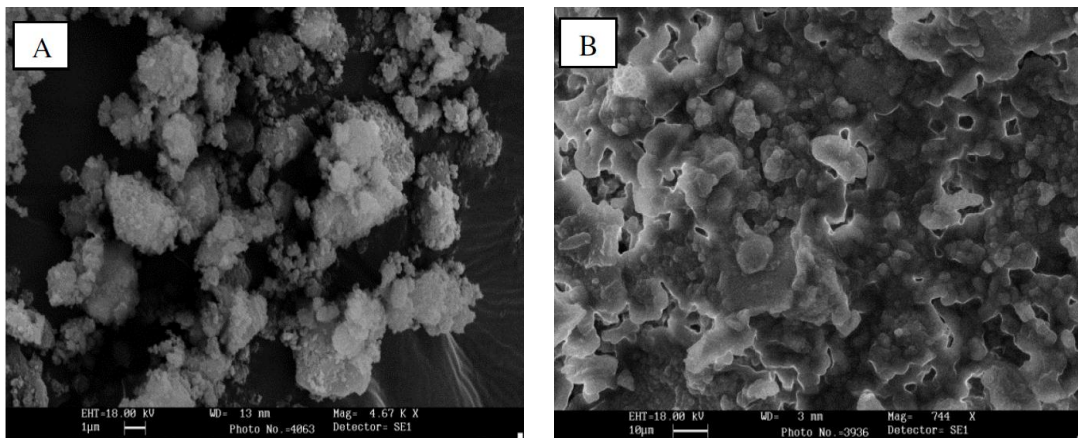


Figure 2. SEM micrographs of the powder mixture milled for 5 h (A) and then heated at 1100 °C for 3 h (B).

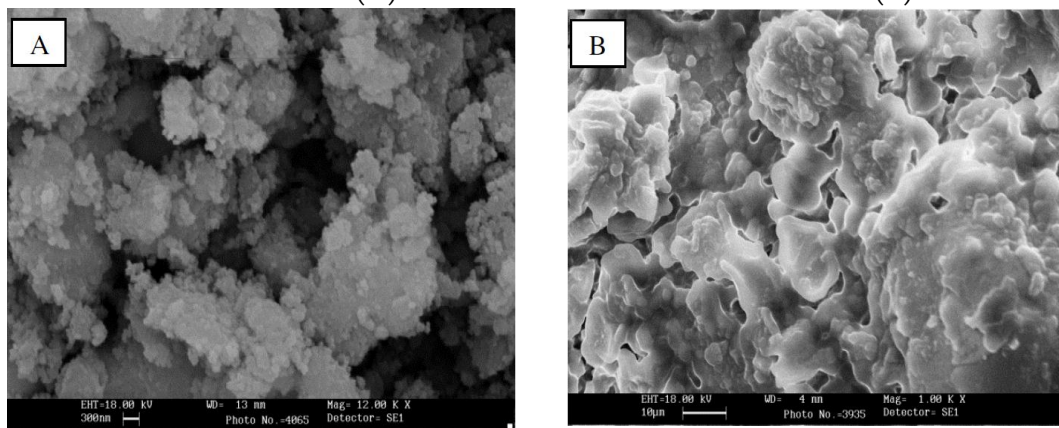


Figure 3. SEM micrographs of the powder mixture milled for 10 h (A) and then heated at 1100 °C for 3 h (B)

Considering SEM micrographs in figure 2 and 3, particles size average of powder mixture materials is micron range.

3.2. XRD results

Figures 4 and 5 show the XRD patterns of the materials mixture milled heated at three temperatures.

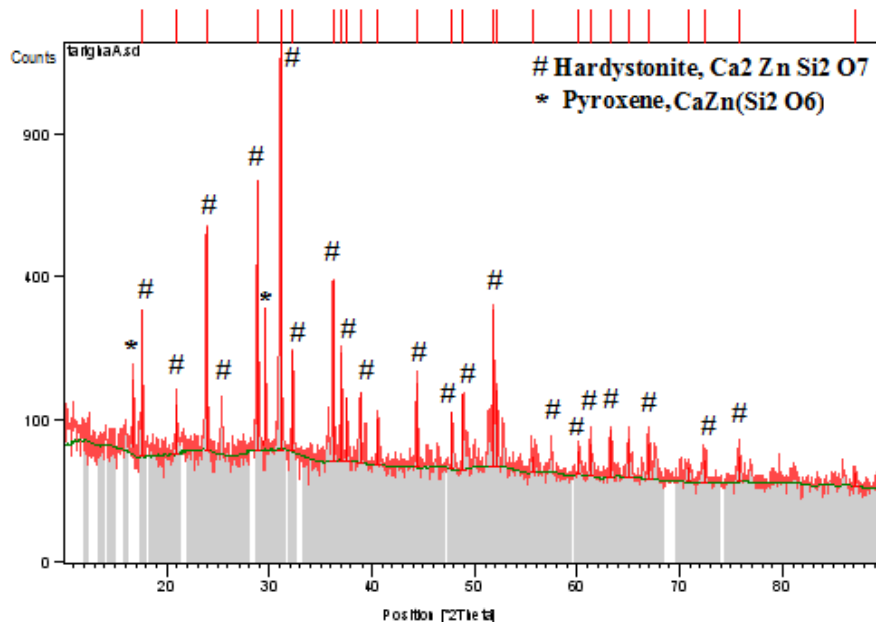


Figure 4. XRD pattern of the materials mixture milled for 5 h and then heated at 1100 °C for 3 h.

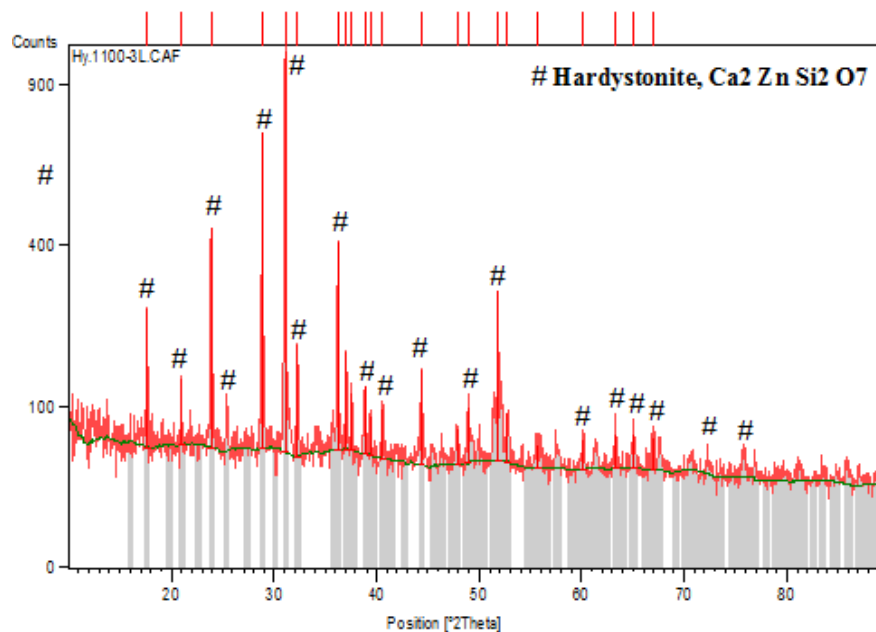


Figure 5. XRD patterns of the materials milled for 10 h and then heated at 1100 °C for 3 h

3.3. Estimation of crystal size

The modified Scherrer equation can provide the advantage of decreasing the sum of absolute values of errors, $\sum(\pm \Delta \ln \beta)^2$, and producing a single line through the points to give a single value of intercept $\ln(K\lambda/L)$.

At this sample, **Figure 6**, the linear regression plot is obtained as $y = -0.7214x - 5.8252$. This is equivalent to $\ln \beta = \ln(1/\cos \theta) + \ln(K\lambda/L)$. As you know, K (shape factor) and λ (XRD radiation wavelength) are 0.89 and 1.54 Å, respectively. From this line, the intercept is -5.8252 and $e^{-5.8252} = K\lambda/L$ and $L = 460 \text{ \AA} = 46 \text{ nm}$ ($L =$ crystal size average). So, crystal size average of Hardystonite synthesized is almost 46 nm.

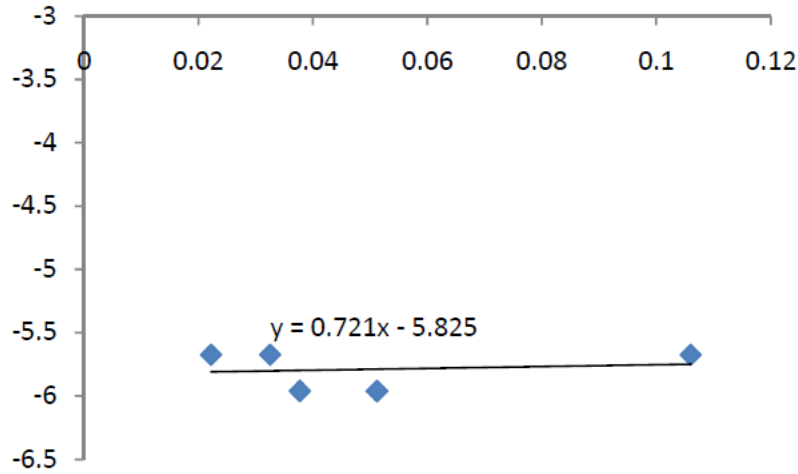


Figure 6. Plot of $\ln \beta$ vs. $\ln (1 / \cos \theta)$ of sample milled for 10 h and heated at 1100 °C, 3 h.

3.4. Energy transfer analysis

Considering the results of optimization, Table 1, is presented for the object of minimum cost function, $W_v = 1.32W_p$. It means that the vial spinning rate should be higher than the plate spinning rate (in the opposite direction). On the other hand, $\varepsilon = 0.398$ which means that the ball size distribution is close to 40 %. The number of ball categories, s , is thus:

$$N_b = 3 \text{ and } \varepsilon = 0.4 \implies s = \text{Integer}(0.4 \times 3) = 1. \quad (10)$$

According to balls size and above interpretation one can write:

$$d_b = 10, N_b = 3, S = 1 \implies (3 \times 10) = 30. \quad (11)$$

So we can say that the size of balls used in proposed design should be 10 mm for the maximum energy transfer to the raw materials.

According to the ball mill parameters given in the **Table 1** and Eq. (6), it was concluded that the energy transfer by the planetary mill per gram of the materials mixture for 5 and 10 h milling time are:

$$E_{t/g} = 5.6 \text{ MJ / g for 5 h (milling time)}$$

and

$$E_{t/g} = 11.2 \text{ MJ / g for 10 h (milling time).}$$

Table 1. The milling parameters optimized values in planetary ball mill.

Symbol	Milling parameters	Optimized values
N_b	Number of balls	3
d_b	Balls diameter (m)	0.01
R_v	Vial radius (m)	0.035
H_v	Vial height (m)	0.07
ε	Ball size distribution coefficient	0.398
W_p	Velocity of the plate (rad / s)	62.8
W_v	Velocity of vial (rad / s)	82.89
R_p	Distance between the center of the plate and the center of the vial (m)	20.0

3.5. Powder density

Real density or pure density of the Hardystonite powder was calculated by Pycnometer. Considering to this method pure density was 2.97 g/cm^3 .

3.6. BET result

The specific surface area of the prepared powder was calculated from the N_2 gas adsorption isotherms using the multipoint BET technique. The average particle size of the prepared powder, assuming that the particles synthesized were spheroid, was calculated as shown in Eq. (12):

$$D = 6000 / (S_{\text{BET}} d), \quad (12)$$

where, d and D are true density (g/cm^3) and the average particle size (micron) of materials mixture milled, respectively. The specific surface area determined by BET was $7.1 \text{ m}^2/\text{g}$, and pure density calculated by Pycnometer method was 2.97 g/cm^3 . So, according to Eq. (12) the particles size was estimated about 285 nm. In fact, the powder mixture is sub-micron size. In addition, it is confirmed in SEM micrograph (**Figure 3**). So, particle size calculated is similar to particle size observed in SEM micrograph. Therefore, calculated particles size, by assuming that the synthesized particles are spheroid in Eq. (12), is acceptable. In fact, most of the particles are spheroid.

4. Discussion

According to the XRD patterns, Hardystonite phase was synthesized in both the samples (**Figures 4** and **5**). But, there is single phase, Hardystonite, just the sample milled for 10 h (**Figure 5**).

In addition, synthesis of Hardystonite phase is affected by using mechanical activation. In fact, mechanical activation intense the syntheses of Hardystonite phase in the sample. In addition, Hardystonite crystal size average is almost 46 nm. Based on energy transfer analysis, the mechanical energy amount transferred to the starting materials mixture is almost 11.2 MJ/g for 10 h milling time. This energy causes the synthesis temperature of Hardystonite reduces to $1100 \text{ }^\circ\text{C}$.

Most of energy transferred to particles materials save in the materials as crystal defects such as grain boundary, dislocations density and vacancy concentration. These crystal defects lead to high path atom diffusely. These high paths causes increasing and intensity of chemical reaction and improvement of Hardystonite phase synthesis. In fact, it causes the synthesis temperature of Hardystonite reduces to low temperature, $1100 \text{ }^\circ\text{C}$.

According to calculation by BET result and SEM micrographs observation, most of the powder particles milled for 10 h are spheroid. In fact, the morphology of powder milled is spheroid and about 285 nm. In fact, the powder mixture is sub-micron size. Moreover, raw materials milled sub-micron particles size, high of specific surface area, lead to increasing of free energy. This high free energy causes driving force to react between raw materials particles. Surface to bulk atoms ratio of particles, SBR, increases by increasing specific surface area of particles size. Regarding to surface diffusion activation energy in comparison bulk diffusion activation energy is too low amount. So, atom diffusion increases between particles and it causes to intensive reaction between raw materials and lead to Hardystonite phase synthesis at low temperature, low thermal energy, after milling for 10 h by high energy ball mill.

5. Conclusions

According to above discussion, we can conclude:

1. Hardystonite nano crystallite, about 46 nm, has been synthesized at 1100 °C by starting materials mixture mechanical activated for 10 h. Whereas, based on the previous studies, Hardystonite phase was synthesized above 1100 °C.
2. According to calculation by BET result and SEM micrographs observation, most of the powder particles milled for 10 h are spheroid. In fact, the morphology of powder milled is spheroid.
3. Based on energy transfer analysis, the energy amount transferred to mixture materials is almost 11.2 MJ/g for 10 h milling time. This energy causes the materials to be mechanically activated.
4. In fact, the energy transferred to the materials mixture (11.2 MJ/g), causes the synthesis temperature of Hardystonite reduces to 1100 °C.

References

1. T. Kokubo, S. Ito, M. Shigematsu, S. Sakka, T. Yamamuro. *J. Mater. Sci.*, 1987, 22, 4067-4070.
2. T. Kokubo. *J. Non-Cryst. Solids*, 1990, 120, 138-151.
3. Y. Abe, T. Kokubo, T. Yamamuro. (1990) *J. Mater. Sci. Mater. Med.* 1 , 233-238.
4. P. Li, Ohtsuki C., Kokubo T., K. Nakanishi, N. Soga, T. Nakamura, T. Yamamuro. *J. Appl. Biomater.*, 1993, 4 , 229-230.
5. WHO Expert Committee on Trace Element in Human Nutrition. Trace elements in human nutrition. WHO Tech. Rep. Ser., 1973, 532, 9-15.
6. Yamaguchi M., Oishi H., Suketa Y., (1998) *Biochem. Pharmacol*, 37, 4075-4080.
7. Ch. Wu, Ch. J., W. Z. *Ceramics Int.*, 2005, 31, 27-31.
8. P. N. Deaza, F. Guitian, S. Deaza. *Scr. Metall. Mater.*, 1994, 31, 1001-1005.
9. K. L. Lin, W. Y. Zhai., S. Y. Ni, J. Chang, Y. Zeng, W. J. Qian. *Ceram. Int.*, 2005, 31, 323-326.
10. Z. R. Gou, J. Chang, W. Y. Zhai. *J. Eur. Ceram. Soc.*, 2005, 25, 1507-1514.
11. C. T. Wu, J. Chang, J. Y. Wang, S. Y. Ni, W. Y. Zhai. *Biomaterials*, 2005, 26, 2925-2931.
12. C. T. Wu, J. Chang. *J. Biomater. Appl.*, 2006, 21, 119-129.
13. M. Yamaguchi. *Trace Elem. Exp. Med.*, 1998, 11, 119-135.
14. C. T. Wu, Y. Ramaswamy, J. Chang, J. Woods, H. Zreiqat. *J. Biomed. B*, 2008, 87, 346-353.
15. M. L. Zhang, W. Y. Zhai, J. Chang. *J. Mater. Sci. Mater. Med.*, 2010, 21, 1169-1173.
16. C. T. Wu, J. Chang, W. Y. Zhai. *Ceram. Int.*, 2005, 31, 27-31.
17. Y. Ramaswamy, C. T. Wu, H. Zhou, H. Zreiqat. *Acta Biomater.*, 2008, 4, 1487-1497.
18. H. X. Lu, N. Kawazoe, G. P. Chen, X. G. Jin, J. Chang. *J. Biomaterials. Appl.*, 2010, 25, 39-56.
19. A. Minshi, M. R. Foroughi, M. R. Monshi. Modified Scherrer equation to estimate more accurately nano-crystallite size using XRD. *World J. Nano Sci. & Eng.*, 2012, 2, 3, 154-160.
20. M. Abdellahi, M. Bahmanpour. A novel technology minimizing the synthesis time of nano structured powders in planetary mills. *Mater. Res.*, 2014, 17, 3, 7-22.